HHS Public Access

Author manuscript

*J Neurochem*. Author manuscript; available in PMC 2016 April 01.

Published in final edited form as:

*J Neurochem*. 2015 April ; 133(2): 174–186. doi:10.1111/jnc.13029.

# Valproic acid induces neuronal cell death through a novel calpain-dependent necroptosis pathway

**Dominique Bollino**, **Irina Balan**, and **Laure Aurelian**[1]

Department of Pharmacology, University of Maryland, Baltimore, Maryland, 21201

## Abstract

A growing body of evidence indicates that valproic acid (VPA), a histone deacetylase (HDAC) inhibitor used to treat epilepsy and mood disorders, has HDAC-related and -unrelated neurotoxic activity, the mechanism of which is still poorly understood. We report that VPA induces neuronal cell death through an atypical calpain-dependent necroptosis pathway that initiates with downstream activation of c-Jun N-terminal kinase 1 (JNK1) and increased expression of receptor-interacting protein 1 (RIP-1) and is accompanied by cleavage and mitochondrial release/nuclear translocation of apoptosis-inducing-factor (AIF), mitochondrial release of Smac/DIABLO, and inhibition of the anti-apoptotic protein X-linked inhibitor of apoptosis (XIAP). Coinciding with AIF nuclear translocation, VPA induces phosphorylation of the necroptosis-associated histone H2A family member H2AX, which is known to contribute to lethal DNA degradation. These signals are inhibited in neuronal cells that express constitutively activated MEK/ERK and/or PI3-K/Akt survival pathways, allowing them to resist VPA-induced cell death. The data indicate that VPA has neurotoxic activity and identify a novel calpain-dependent necroptosis pathway that includes JNK1 activation and RIP-1 expression.

### Keywords

HDAC inhibitors; H2AX; AIF; calpain; necroptosis; PCD

## INTRODUCTION

Valproic acid (VPA) is a histone deacetylase (HDAC) inhibitor used to treat epilepsy and mood disorders. Its utility as an anticonvulsant that blocks voltage-dependent sodium channels was originally supported by clinicians, but subsequently challenged due to its side-effects and HDAC-dependent and-independent toxicity (Chateauvieux *et al*. 2010, Han *et al*. 2013, Shah *et al*. 2013). While protection was reported in some neurological disease studies (Chen *et al*. 2014, Carriere *et al*. 2014, Zhang *et al*. 2014), VPA-induced neurodegeneration was seen in both cultured neuronal cells and experimental animals (Jin *et al*. 2005, Yochum *et al*. 2008, Umka *et al*. 2010, Tung & Winn 2011, Fujiki *et al*. 2013). VPA reduced the proliferation of hippocampal neurons and caused cognitive impairment in intraperitoneally injected rats (Umka et al. 2010) and neonatal mice and rats given clinically relevant doses of

[1]To whom correspondence should be addressed. laurelia@umaryland.edu.

The authors declare no conflicts of interest.

anticonvulsant VPA therapy exhibited widespread apoptotic neurodegeneration in several brain regions (Bittigau *et al*. 2003, Yochum et al. 2008). In humans, VPA has established teratogenic activity. It causes neural tube defects and increases the incidence of children with autism spectrum disorder (ASD), when taken during pregnancy (Arndt *et al*. 2005, Christensen *et al*. 2013). Developmental neurotoxicity was attributed to the generation of free radicals, oxidative stress (Chaudhary & Parvez 2012) and caspase-dependent apoptosis (Sheikh *et al*. 2010a, Sheikh *et al*. 2010b, Fujiki et al. 2013), and the morphological changes seen in the brains of autistic children confirmed that VPA induces programmed cell death (PCD) (Sheikh et al. 2010a, Sheikh et al. 2010b). The pathways involved in the VPA-induced neurotoxicity are still poorly understood (Johannessen 2000). Caspase-independent PCD was also reported (Forgione & Tropepe 2011), but its exact mechanism is still unknown. We report, for the first time, that VPA induces a cascade of deleterious events, which contribute to neuronal cell death through an atypical calpain-dependent necroptosis pathway. The pathway involves early activation of c-Jun-N-terminal kinase 1 (JNK1) and increased expression of receptor-interacting protein 1 (RIP-1), and is followed by cleavage/nuclear translocation of apoptosis-inducing-factor (AIF) and phosphorylation of the histone H2A family member H2AX as well as the altered balance between the death-inducing protein Smac/DIABLO and the protective protein XIAP.

## MATERIALS AND METHODS

### Cells and neuronal differentiation

PC12 cells were grown in DMEM/F12 medium (Media Tech, Herndon, VA, USA) with 10% FBS, 0.36% D-glucose (Sigma-Aldrich, St. Louis, MO, USA), and 0.009% gentamicin (Invitrogen, Waltham, MA USA. The establishment and properties of stably transfected PC12 cells (PC47 and PC70) that have constitutively activated survival pathways were previously described (Wales et al., 2008). For neuronal differentiation, the cells were cultured (4 days) on rat tail collagen-coated cover glass or polystyrene flasks and grown in NeuroBasal medium with 2 mmol/L L-glutamine, B-27 supplement, 0.009% gentamicin (Invitrogen) and 100 ng/mL nerve growth factor (NGF,2.5S; Millipore, Billerica, MA, USA). Fresh NGF was supplied every other day. Differentiation was confirmed by the formation of neurites and staining with antibody to the neuronal differentiation marker MAP-2 (Sano *et al*. 1990), as previously described (Wales *et al*. 2008). We confirmed neuronal differentiation and its failure to alter transgene expression and similar results were obtained when differentiation was for 4, 7 or 12 days (SD, Fig S1). Primary rat cortical neurons were purchased from Life Technologies (Grand Island, NY). They were cultured on poly-D-lysine coated polystyrene plates and grown in NeuroBasal medium with 0.5mM GlutaMAX supplement and 2% B-27 supplement (Life Technologies), as per manufacturer's instructions.

### Antibodies and reagents

Antibodies to XIAP, RIP-1, phosphorylated JNK, and phosphorylated H2AX were purchased from Cell Signaling Technology (Danvers, MA, USA). Antibodies to actin, GAPDH, AIF, Smac/DIABLO, and calpain were purchased from Santa Cruz Biotechnology (Santa Cruz, CA, USA). The calpain inhibitor PD150606 was purchased from Calbiochem

(La Jolla, CA, USA), the pancaspase inhibitor z-VAD-fmk and necroptosis inhibitor necrostatin-1 (Nec-1) from Sigma-Aldrich (St. Louis, MO, USA) and the Ambion Silencer Select RIP-1 siRNA from Life Technologies. It was transfected into neuronally differentiated PC12 cells using Lipofectamine RNAiMAX Reagent (Life Technologies) as per manufacturer's instructions. Alexafluor 488-conjugated anti-goat secondary antibody was purchased from Invitrogen (Carlsbad, CA, USA) and horseradish peroxidase-conjugated anti-rabbit and anti-mouse antibodies from Cell Signaling Technologies.

## Cell death

Cell death was determined by trypan blue and ethidium homodimer staining. For trypan blue staining, an aliquot of the cell suspension was incubated with an equal volume of 0.4% trypan blue and the percentage of dead cells (identified by blue staining) was calculated relative to the total cell numbers in 4 independent fields using a hemacytometer. For ethidium homodimer staining, cells were incubated with ethidium homodimer (Life Technologies) for 30 min at room temperature according to the manufacturer's instructions, mounted in Vectashield with DAPI (Vector,Burlingame, CA, USA) and visualized with an Olympus BX50 fluorescent microscope (Center Valley, PA, USA). Staining cells were counted in four randomly selected fields, for a total of at least 250 cells. Propidium iodide staining was also used for cell death confirmation, as described in Supplemental data (SD) (Fig. S3).

## Cytoplasmic and nuclear separation and Immunoblotting

Cytoplasmic and nuclear fractions were separated as previously described (Wales et al. 2008). Briefly, cell pellets were suspended in 50 mM Tris-Hcl buffer (pH 8.0) with 50 mM NaCl, 1% NP-40, 1 mM dithiothreitol and protease inhibitors on ice. The cells were centrifuged (7000 g; 1 min) and the resulting supernatant (cytoplasmic fraction) was removed. The nuclear pellet was resuspended in the same buffer but with 450 mM NaCl and sonicated until in solution. For whole cell extraction, cell pellets were lysed with radioimmunoprecipitation buffer [20 mM Tris-HCl (pH 7.4), 0.15 mM NaCl, 1% Nonidet P-40 (Sigma), 0.1% sodium dodecyl sulfate (SDS), 0.5% sodium deoxycholate] supplemented with protease and phosphatase inhibitor cocktails (Sigma). Protein concentrations were determined using the bicinchoninic assay (Pierce, Rockford, IL, USA) and 50μg of extracts were resolved using SDS-PAGE and transferred onto PVDF membranes. Membranes were blocked for 1 hour in TNT buffer [0.01 M Tris-HCl (pH 7.4), 0.15M NaCl, 0.05% Tween 20] containing 5% milk or bovine serum albumin (Sigma-Aldrich). They were incubated with primary antibody overnight at 4°C, followed by incubation with secondary antibodies conjugated to horseradish peroxidase. Quantitation was performed by densitometric scanning with the Bio-Rad GS-700 imaging densitometer (Bio-Rad, Hercules, CA, USA). The results of three independent experiments are expressed as the mean actin or GAPDH-adjusted densitometric units ± SE.

## Immunofluorescent staining

Cells were fixed with 4% paraformaldehyde (30 min; room temperature (RT)) and permeabilized (2 min; 4°C) with 0.1% Triton X-100 in 0.1% sodium citrate buffer. They were incubated with primary antibody diluted in 5% bovine serum albumin and 5% normal

goat serum in PBS overnight at 4°C, washed in phosphate-buffered saline (PBS) with 0.1% Tween 20 and exposed to fluorochrome-labeled secondary antibodies (1 h; 37°C). Slides were mounted in Vectashield with DAPI (Vector) and visualized with an Olympus BX50 fluorescent microscope (Center Valley, PA, USA). Staining cells were counted in four randomly selected fields, for a total of at least 250 cells. When used, Mitotracker Red 580 was added to cells (30 min, 37°C) as per manufacturer's instructions prior to fixation with paraformaldehyde.

### Statistical analysis

Analysis of variance (ANOVA) was carried out using SigmaPlot 11.0 for Windows. One-way analysis of variance was followed by pairwise comparison with the Holm-Sidak test.

## RESULTS

### VPA has dose-dependent neurotoxic activity

The ability of VPA to cause neuronal cell death was examined in neuronally differentiated PC12 cells, which are an established model for the study of neuronal cell life/death decisions (Francois *et al*. 2001, Valavanis *et al*. 2001). PC12 cells were differentiated by 4 days of culture with NGF and differentiation was confirmed by the formation of neurites and expression of the neuronal differentiation marker MAP-2 (SD, Fig. S2). A first series of experiments to examine the effect of VPA on neuronal cells followed on previous findings that the levels of VPA in the serum from treated patients is generally 0.2–0.6 mM, but fetuses may be exposed to up to 5 times higher levels in maternal serum at term (Ornoy 2009). Accordingly, the neuronally differentiated PC12 cells were treated with VPA (0.05 to 5.0 mM) or mock-treated with PBS and examined for cell death by ethidium homodimer staining at 3 and 5 days post-treatment. Results are expressed as % dead cells normalized to the untreated cultures (% dead cells in VPA-treated cultures - % dead cells in the untreated cultures). The data summarized in Fig. 1A indicate that VPA caused dose-dependent cell death with relatively low numbers of dead cells (20%) seen at 0.05–0.5mM and higher percentages (35–50%) seen at 1 and 5mM concentrations. Similar results were obtained by trypan blue staining (data not shown). We used the 1mM concentration in the subsequent experiments, because: (i) the therapeutically relevant dose is lower than 5mM (Ornoy 2009), and (ii) previous studies using 1mM VPA reported contradictory cell type-dependent effects, with caspase-dependent apoptosis seen in non-neuronal cells (Dragunow *et al*. 2006, Wang *et al*. 2011) and protection from cell death seen in neurons (Kanai *et al*. 2004). Significantly, VPA-induced cell death was also seen in similarly treated human neuroblastoma SK-N-SH cells (SD, Fig. S3A) as measured by propidium iodide staining (SD, Fig. S3B) and in primary rat cortex neuronal cultures (26.8 ± 0.54% and 1.8 ± 0.27% cell death for VPA as compared to mock-treated cultures) (Fig 1C). Collectively, the data indicate that VPA induced cell death is not a technical artifact resulting from the use of PC12 cells or a specific assay and it extends to human neuronal cell lines and primary neuronal cultures. However, VPA-treated cells were negative for TUNEL staining (SD, Fig. S3C), suggesting that death is not caused by apoptosis.

### Activated survival pathways block VPA-induced neurotoxicity

To confirm the specificity of the VPA neurotoxic effect, PC12 cells stably transfected with the herpes simplex virus type 2 protein ICP10PK (PC47 and PC70) that have constitutively activated PI3-K/Akt and MEK/ERK survival pathways (SD, Fig. S1] and resist death induced by various toxic stimuli (Perkins *et al*. 2003, Gober *et al*. 2006, Laing *et al*. 2006, Golembewski *et al*. 2007, Wales et al. 2008), were studied in parallel. PC47 and PC70 cells were differentiated by 4 days of culture with NGF as described for PC12 cells and differentiation was again confirmed by the formation of neurites and expression of the neuronal differentiation marker MAP-2 (SD, Fig. S2). Differentiated PC47, PC70 and PC12 cells were treated with VPA (1mM) and assayed for cell death by trypan blue staining at 1, 2, 3 and 5 days post treatment. Results are expressed as % dead cells normalized to the untreated cultures. VPA caused time-dependent cell death in PC12 cells that reached maximal levels on days 3–5 post-treatment, but cell death was not seen in PC47 and PC70 cells (Fig. 1B), indicating that activated MEK/ERK and/or PI3-K/Akt survival pathways counteract the ability of VPA to induce cell death.

### Calpain, JNK, and necroptosis inhibitors block VPA-induced cell death

Having seen that VPA-treated cultures are TUNEL negative, we wanted to better understand the mechanism of the VPA-induced cell death. Duplicate cultures of neuronally differentiated PC12 cells were treated with VPA (1mM) in the absence or presence of the pancaspase inhibitor z-VAD-fmk (100μM), the calpain inhibitor PD150606 (100μM), the JNK inhibitor SP600125 (10μM) or Necrostatin-1 (Nec-1; 50μM), a potent inhibitor of the RIP-1 kinase activity involved in necroptosis (Degterev *et al*. 2008). They were examined for cell death by trypan blue staining at 1, 2, 3, and 5 days post-treatment and the results are expressed as % inhibition calculated as 100-((% death with inhibitors/% death without inhibitors) x100), normalized to untreated cultures. The data are summarized in Fig 1D. Consistent with the absence of TUNEL staining (SD, Fig. S3C), z-VAD-fmk did not interfere with the ability of VPA to induce cell death, suggesting that death is not caspase-dependent. This is also consistent with the absence of caspase activation as shown for caspases-3 and -8 in SD Fig. S4. However, cell death was inhibited in cultures that were given VPA together with PD150606, SP600125 or Nec-1, with maximal inhibitory levels seen on days 3 post-treatment. Maximal inhibition (relative to cultures given VPA alone) was seen for PD150606 [63 ± 0.97% ($P= 0.003$) and 82.3 ± 2.8%; ($P<0.001$) on days 2 and 3 post-treatment, respectively] followed by Nec-1 [50 ± 1.1 % ($P=0.014$) and 69.6 ± 4.5% ($P\leq 0.001$) on days 2 and 3 post-treatment, respectively]. The inhibitory levels seen for SP600125 were similar on days 2 and 3 post-treatment (41.5 ± 3.1%; $P<0.01$), but inhibition was virtually absent at 5 days post-treatment. Collectively, the data indicate that VPA-induced cell death is through calpain and JNK activation and includes Nec-1 inhibitable necroptosis. We conclude that the VPA-induced cell death mechanism observed in PC12 cells is applicable to primary neuronal cultures, because PD150696, but not z-VAD-fmk, was also able to significantly ($P<0.001$) inhibit cell death in VPA-treated primary neurons (53.1 ± 2.3% inhibition) (Fig. 1E).

### Calpain is activated in VPA-treated PC12, but not PC47 cells

Having seen that the VPA-induced death of neuronally differentiated PC12 cells is significantly reduced by treatment with PD150606, we wanted to confirm that VPA causes calpain activation. Protein extracts from neuronally differentiated PC12 and PC47 cells treated or not with VPA (1mM; 48hrs) were immunoblotted with antibody to the p28 calpain regulatory subunit, the disappearance of which is indicative of activation (Goll *et al*. 2003). Cells similarly treated with VPA in the absence or presence of PD150606 (100M), Nec-1 (50M) or SP600125 (10M) were studied in parallel and the blots were stripped and re-probed with GAPDH antibody used as loading control. The expression levels were determined by densitometric scanning, as described in MM and the results are summarized in Fig. 2. p28 was expressed in the mock-treated PC12 cells, but expression was virtually lost upon VPA treatment, indicative of calpain activation. Consistent with this interpretation, the levels of p28 in PC12 cells given VPA together with PD150606 were restored to those seen in the mock-treated cells, but this was not the case in cells given VPA together with SP600125 or Nec-1. The levels of p28 were not reduced in VPA-treated PC47 cells, indicating that VPA does not activate calpain in these cells and confirming that its ability to induce cell death is through calpain activation.

### Calpain-mediated JNK1 activation contributes to VPA-induced cell death

JNKs have received considerable attention in the context of apoptosis-related neurodegeneration (Coffey 2014), but their contribution to VPA-induced neurotoxicity, if any, is unclear. Following on the finding that SP600125 inhibits VPA-induced cell death in neuronally differentiated PC12 cells (Fig. 1), we wanted to better understand the role of JNK activation in the death process. Moreover, because PC12 cells do not express the JNK3 isoform (Mielke *et al*. 2000) that had been previously associated with apoptosis in neurons (Waetzig & Herdegen 2003), our system provides a unique opportunity to verify the differential, context-specific role of the JNK1/2 isoforms in neuronal cell death.

Neuronally differentiated PC12 and PC47 cells were mock-treated or treated with VPA (1mM; 48hrs) and protein extracts were immunoblotted with an antibody that recognizes the phosphorylated (activated) JNK 1 and 2 isoforms (pJNK1 and pJNK2, respectively). The blots were stripped and re-probed with antibody to total JNK, used as control. Mock-treated PC12 cells had minimal levels of pJNK1 and pJNK2. VPA caused a significant increase in the levels of pJNK1, but not pJNK2, indicating that it has an isoform-specific activity. This activity is calpain-dependent, because the levels of pJNK1 were not increased in cells given VPA together with PD150606 (100 μM), and the levels of pJNK1 in PC12 cells given VPA together with Nec-1 (50 μM) were similar to those in cells given VPA alone. VPA did not increase pJNK1 levels in PC47 cells that resist cell death (Fig. 3A). Collectively, the data indicate that: (i) VPA specifically activates JNK1, (ii) JNK1 activation is calpain-dependent and upstream of Nec-1 inhibitable necroptosis and (iii) JNK1 activation is associated with VPA-induced cell death.

### VPA induces RIP-1 expression through calpain/JNK1 activation

Cell death activated when caspase-dependent apoptotic pathways are inhibited is also known as “necroptosis”. Recent studies have shown that necroptosis requires the serine-threonine

kinases RIP-1 and RIP-3, and results from overproduction of reactive oxygen species (ROS) and eventual mitochondrial dysfunction (Festjens *et al*. 2007, Cho *et al*. 2009, Vandenabeele *et al*. 2010). Nec-1 is a selective inhibitor of RIP1 kinase activity (Degterev et al. 2008) and thereby, necroptosis.

Having seen that Nec-1 inhibits VPA-induced cell death in PC12 cultures, we wanted to better understand the relationship between the VPA-induced cell death and RIP-1. Neuronally differentiated PC12 cells were mock-treated or treated with VPA (1mM; 48 hrs) alone or together with PD150606 (100 μM), SP600125 (10 μM), or Nec-1 (50 μM), and protein extracts were immunoblotted with RIP-1 antibody. The blots were stripped and re-probed with antibody to GAPDH used as loading control. The levels of RIP-1 were increased in the VPA-treated as compared to untreated PC12 cells, but increased expression was not seen in cell given VPA together with PD150606 or SP600125 (Fig. 3B). The levels of RIP-1 were not altered in PC12 cells given VPA together with Nec-1, which inhibits the RIP-1 kinase activity (Degterev et al. 2008, Han *et al*. 2012) and VPA did not alter RIP-1 expression in PC47 cells (Fig. 3B) that resist VPA-induced cell death. Similar results were obtained at 72 hrs post treatment (data not shown). The data indicate that VPA induces RIP-1 expression through a calpain/JNK1 pathway that is activated at 2–3 days post-treatment, and this increased expression contributes to the VPA-induced cell death.

While we did not examine the effect of VPA on RIP-1/RIP-3 complexation, our data confirm that inhibition of RIP-1 expression (and thereby kinase activity) causes a significant decrease in VPA-induced cell death. Specifically, neuronally differentiated PC12 cells were treated (2 days) with a RIP-1 siRNA-Lipofectamine complex, given VPA (1mM) and examined for cell death by trypan blue staining at 2 and 3 days later. Cell death was inhibited when VPA was given together with RIP-1 siRNA [34.6 ± 2.4 % and 57.8 ± 3.3 % inhibition on days 2 and 3, respectively ($P<0.001$)] (Fig. 3C) and these levels are similar to those seen for Nec-1 inhibition (Fig. 1C). The effect of the RIP-1 siRNA on cell death was due to RIP-1 knockdown, as confirmed by immunoblotting of cell extracts from duplicate cultures given VPA+ siRNA for 2 or 3-days (Fig 3D).

### VPA induces calpain-dependent AIF cleavage and nuclear translocation

Mitochondrial release of several pro-apoptotic molecules is a determining factor for inducing caspase-dependent and independent cell death (Xiong *et al*. 2014). We focused on apoptosis inducing factor (AIF) because it is cleaved by calpain to a 57kDa product (tAIF), which is released from the mitochondria (Cao *et al*. 2007) and translocates to the nucleus where it triggers DNA degradation (Sevrioukova 2011) and provokes necroptosis (Delavallee *et al*. 2011). Neuronally differentiated PC12 and PC47 cells were mock-treated or treated with VPA (1mM) alone or together with PD150606 (100 μM). Total cell extracts were obtained at 72 hrs post-treatment and cytoplasmic and nuclear fractions were generated as described in MM. They were immunoblotted with AIF antibody and the blots were stripped and re-probed with actin antibody used as loading control. The total cell extracts from the mock-treated PC12 cells had relatively low levels of a 57 kDa band that is consistent with tAIF (Cao et al. 2007), but the levels were significantly higher in the VPA-treated PC12 cells. The levels of tAIF in PC12 cells that received VPA together with

PD150606 were similar to those in the untreated cells (Fig. 4A), indicating that VPA induces calpain-dependent AIF cleavage. Immunoblotting of the cytoplasmic and nuclear fractions from the untreated and VPA-treated PC12 cells confirmed that VPA causes a significant increase in the levels of tAIF and it translocates to the nucleus (Fig. 4B). Similar analysis of the cytoplasmic and nuclear fractions from the untreated and VPA-treated PC47 cells indicated that the levels of tAIF were minimal in both fractions and they were not increased by treatment with VPA (Fig. 4B). It should be pointed out that tAIF was not seen in PC12 cells examined at 2 days post treatment with VPA, suggesting that AIF cleavage is a relatively delayed VPA-induced process (initiates on day 3 post-treatment) (Fig. 1).

To further confirm the contribution of tAIF mitochondrial release and nuclear translocation to VPA-induced cell death, neuronally differentiated PC12 cells mock-treated or treated with VPA (1mM, 72hrs) alone or together with PD150606 (100 μM) were stained in double immunofluorescence with Alexa Fluor 488-labeled AIF antibody and the mitochondrial selective dye MitoTracker Red 580 in order to confirm its release from the mitochondria and its nuclear translocation. The cells with nuclear staining were counted in 4 randomly selected fields (at least 250 cells) and the results are expressed as % cells with nuclear staining calculated relative to the total cell number determined by DAPI staining. AIF co-localized almost entirely with the mitochondrial stain in mock-treated cells, nuclear staining was seen in 19 ± 2.5 % of the cells in the VPA-treated cultures. PC12 cells given VPA together with PD150606 primarily evidenced AIF/mitochondrial co-localization confirming that calpain cleaves AIF, leading to its mitochondrial release and nuclear translocation (Fig. 5A). tAIF nuclear translocation was not seen in the untreated or VPA-treated PC47 cells (SD, Fig. S5).

### VPA treatment induces H2AX phosphorylation

H2AX, a member of the histone H2A family has an SQE motif in its C-terminal tail that is phosphorylated at Ser139 (γH2AX) and is associated with the generation of DNA double-strand breaks. Once in the cytosol, tAIF translocates to the nucleus where, in cooperation with γH2AX, it provides the lethal DNA-degrading activity characteristic of AIF-mediated necroptosis (Baritaud *et al*. 2010, Pasupuleti *et al*. 2013). Having seen that VPA-induces AIF cleavage and nuclear translocation, we wanted to know whether this is accompanied by increased levels of H2AX. Duplicate PC12 cultures untreated or treated with VPA (1mM) were stained with H2AX antibody at 3 days post-treatment and the % H2AX staining cells was calculated as described for tAIF. Staining was seen in 21.1 ± 1.2 % of the VPA-treated cells at 3 days post-treatment, a significant increase over the minimal % of staining cells in the untreated cultures ($p < 0.01$) (Fig. 5B). γH2AX staining was not seen in the untreated and VPA-treated PC47 cells (Fig. S5). Significantly, γH2AX staining was not increased in cells given VPA for only 2 days, consistent with the interpretation that that γH2AX upregulation, like AIF cleavage/nuclear translocation, is a relatively delayed VPA-induced death process (initiates on day 3 post-treatment). While we did not directly examine the interaction between nuclear tAIF and γH2AX, the data indicate that VPA induces H2AX phosphorylation, likely contributing to necroptosis through tAIF interaction (Baritaud et al. 2010, Pasupuleti et al. 2013).

### VPA alters the Smac/DIABLO vs XIAP balance

Having seen that VPA treatment induces AIF cleavage and mitochondrial release, we wanted to know whether it is also associated with the release of other mitochondrial intermembrane proteins that modulate PCD. We focused on Smac/DIABLO, which inhibits the Inhibitors of apoptosis (IAP) proteins (Morizane *et al*. 2005) because its altered balance relative to the IAP proteins cIAP1 and cIAP2 induces necroptosis (McComb *et al*. 2012, Steinhart *et al*. 2013). Extracts from neuronally differentiated PC12 cells untreated or treated with VPA (1mM, 72hrs) in the absence or presence of PD150606 (100 μM) were immunoblotted with Smac/DIABLO antibody and the blots were sequentially stripped and re-probed with antibodies to X-linked IAP (XIAP) or GAPDH (loading control). A significant increase in the levels of Smac/DIABLO was seen in the VPA-treated cells and it was accompanied by a marked decrease in the levels of XIAP (Fig 6A). PD150606 restored the Smac/DIABLO and XIAP levels to those seen in the untreated cells (Fig. 6B) and a similar effect was not seen in PC47 cells (data not shown). While additional studies are needed in order to fully document the role played by Smac/DIABLO in VPA-induced cell death, our data indicate that VPA causes a calpain-dependent alteration in the Smac/DIABLO vs XIAP balance that is likely to contribute to cell death through the promotion of necroptosis.

## DISCUSSION

VPA is a HDAC inhibitor, the primary indication of which is for the treatment of epilepsy and mood disorders (Leng *et al*. 2008, Chiu *et al*. 2013), apparently due to its ability to enhance GABAergic neurotransmission, modulate brain metabolism, decrease excitability and affect voltage-gated sodium, potassium and calcium channels (Johannessen 2000, Loscher 2002). While VPA was reported to have neuroprotective activity in some models of CNS injury and neurodegenerative disorders (Carriere et al. 2014, Chen et al. 2014, Zhang et al. 2014), a growing body of evidence indicates that it causes HDAC-related and -unrelated neuronal cell death (Han et al. 2013, Shah et al. 2013). Indeed, VPA was shown to exacerbate the death of cerebellar granule neurons (Jin et al. 2005), reduce the proliferation of hippocampal neurons resulting in cognitive impairments (Umka et al. 2010), and induce apoptosis in various neuronal cell populations (Wang et al. 2011, Han et al. 2013, Shah et al. 2013). Rats and mice exposed to VPA *in utero* or shortly after birth present with behavioral and structural abnormalities similar to those observed in humans with ASD (Ingram *et al*. 2000, Yochum et al. 2008). In humans, VPA administration during pregnancy increases the incidence of autism in the born children (Christensen et al. 2013) associated with widespread brain apoptosis (Bittigau et al. 2003, Yochum et al. 2008, Sheikh et al. 2010a, Sheikh et al. 2010b). VPA was also shown to promote caspase-independent neuronal cell death albeit, by an as yet poorly understood mechanism (Forgione & Tropepe 2011). We report, for the first time, that VPA activates a previously unrecognized calpain-dependent necroptosis cascade that initiates with the activation of JNK1/RIP-1 signaling and is followed by AIF cleavage/nuclear translocation and H2AX phosphorylation as well as an altered Smac/DIABLO to XIAP balance, as schematically represented in Fig. 7. The following comments seem pertinent with respect to these findings.

Caspases are universally recognized as the main players in apoptosis (Green 2000, Danial & Korsmeyer 2004). However, it is becoming increasingly evident that death can also be caused by other mechanisms, the relationship of which to apoptosis is still poorly understood. RIP-1, for example, is a core component of the cell death-inducing platform known as ripoptosome, which has a critical role in regulating the switch from caspase-dependent apoptosis to necroptosis. RIP-1 is cleaved by activated caspase-8, thereby directing the cell to undergo apoptosis, but in the absence of caspase activation, RIP-1 can complex with and phosphorylate RIP-3 to initiate necroptosis. Calpains are Ca2+-dependent cysteine proteases that can also be activated by apoptotic stimuli resulting in the cleavage of multiple targets and the mitochondrial release of death-inducing proteins (Storr *et al*. 2011). One of these is the calpain-cleaved AIF protein (tAIF) that translocates to the nucleus and in cooperation with γH2AX, provokes DNA degradation and necroptosis (Baritaud et al. 2010, Cabon *et al*. 2012, Autheman *et al*. 2013, Pasupuleti et al. 2013). Another one of the death-inducing proteins that are released from the mitochondria as a result of calpain activation is Smac/DIABLO that inhibits the anti-apoptotic cIAP proteins, thereby promoting necroptosis (McComb et al., 2012, Steinhart et al., 2013).

We used neuronally differentiated PC12 cells, which are an established model of neuronal cell life/death choices to examine whether VPA causes cell death and define the mechanism responsible for neurotoxicity. PC12 cells modified to resist death-inducing stimuli through constitutive activation of the PI-3K/Akt and MEK/ERK survival pathways (PC47 and PC70; SD, Fig. S1) provide a well-defined cell culture system for the verification of neurotoxic mechanisms, and were studied in parallel. Neuronal differentiation was by exposure to NGF and it was confirmed by neurite formation and expression of the differentiation marker MAP-2 (SD, Fig. S2). As schematically represented in Fig. 7, we found that VPA induced a time-dependent cascade of death signals the outcome of which was maximal levels of cell death on days 3–5 post-treatment. This was determined by different assays including ethidium homodimer, trypan blue and propidium iodide staining and involved a cascade of death-inducing signals. However, TUNEL staining was negative (SD, Fig. S3), caspases were not activated (SD, Fig. S4) and the pancaspase inhibitor z-VAD-fmk did not inhibit cell death, indicating that death is not due to caspase-dependent apoptosis. By contrast, cell death was inhibited by the calpain inhibitor PD150606 and similar results were obtained in primary neurons in which cell death was also inhibited by the calpain but not pancaspase inhibitor. Significantly cell death was also inhibited by the JNK inhibitor SP600125, and immunoblotting experiments confirmed that VPA induces calpain and JNK1 activation, as respectively measured by loss of the p28 calpain regulatory subunit and a significant increase in the levels of phosphorylated JNK1 (pJNK1) relative to those in untreated cells. Both the loss of p28 and the increase in pJNK1 were seen at 2 days of VPA treatment, indicating that they are relatively early events in the VPA-induced cell death and they were not seen in PC47 cells that do not die in response to VPA treatment. Significantly, the levels of pJNK1 were not increased in cells given VPA together with the calpain inhibitor PD150606 and VPA did not increase the levels of pJNK2, indicating that VPA specifically activates JNK1 in a calpain-dependent mechanism and underscoring the differential contribution of the two JNK isoforms. While the JNK isoforms were previously reported to have distinct signaling pathways in neuronal cells (Haeusgen *et al*. 2009, Zhao *et al*. 2012)

and a different impact on behavioral parameters (Reinecke *et al*. 2013), the ability of calpain to specifically activate JNK1 thereby leading to cell death identifies a novel death regulatory process in neurons. JNK activation had previously been shown to occur upstream of calpain activation (Huang *et al*. 2014) or parallel to calpain activation during necrosis (Douglas & Baines 2014). The exact mechanism responsible for calpain-mediated JNK activation is still unclear. Calpain could cleave JNK inhibitory proteins, such as JNK-interacting protein-1 (JIP-1), a scaffold protein and specific inhibitor of JNK, thereby inducing JNK activation. In addition, calpain activation can induce intracellular calcium overload(Lai *et al*. 2014) and it, in turn, can cause JNK phosphorylation(Huang et al. 2014). Indeed, calpains were previously shown to play a central role in the conversion of $Ca^{+2}$ signals from the stressed endoplasmic reticulum to JNK activation (Tan *et al*. 2006). The VPA-induced calpain/JNK1 death pathway is not an artifact of the VPA dose, because at the same dose VPA caused caspase activation in non-neuronal cells (Stockhausen *et al*. 2005, Dragunow et al. 2006, Wang et al. 2011).

The relationship between JNK activation and RIP-1, if any, is still unknown. We found increased expression of RIP-1, in the treated relative to untreated PC12 cultures as early as 2 days post-treatment. RIP-1 upregulation was inhibited by SP600125 indicating that it is JNK1-dependent. This is likely mediated by the activation of the AP-1 transcription factor, which regulates RIP-1 transcription (Christofferson *et al*. 2012). Consistent with this interpretation, Nec-1 did not inhibit the ability of VPA to upregulate RIP-1 expression. We do not believe that death involves the specific activation of TNF/Fas/CD40/CD30 receptor family members (Hirsch *et al*. 2013) that include the NGF-activated p75NGFR receptor in PC12 cells (Mahadeo *et al*. 1994) because the calpain/JNK1/RIP-1 pathway was also associated with cell death in the VPA-treated human neuroblastoma SK-N-SH cells. However, we conclude that increased RIP-1 expression is involved in the VPA-induced cell death, because: (i) expression was blocked by the calpain inhibitor PD150606, which inhibits cell death, (ii) RIP-1 expression was not seen in PC47 cells that resist VPA-induced cell death, (iii) and knockdown of RIP-1 with specific siRNA inhibited cell death. Indeed, both the RIP-1 siRNA and Nec-1 inhibited cell death beginning on day 2 post-treatment and inhibition reached maximal levels one day later (day 3 post-treatment), likely reflecting the ability of Nec-1 to specifically inhibit RIP-1 kinase activity. Since RIP-1 is a caspase-8 substrate (Lin *et al*. 1999), its increased levels in the VPA-treated PC12 cells are likely favored by the failure to induce caspase activation, potentially indicative of cell type and context specific effects of VPA-induced neurotoxicity.

Interestingly, beginning on day 3 post-treatment, the VPA-treated PC12 cells also evidenced calpain-dependent AIF cleavage and mitochondrial release of tAIF, with increased tAIF levels seen in both the cytoplasm and nuclear fractions relative to untreated cells. This increase was due to calpain-mediated mitochondrial release, as confirmed by staining with the mitochondrial selective dye MitoTracker Red 580, and it was blocked by treatment with the calpain inhibitor PD150606. Significantly, the tAIF nuclear translocation coincided temporally with VPA-induced γH2AX increase, the association of which with tAIF is known to create a DNA-degrading complex that provokes chromatinolysis and cell death by necroptosis (Artus *et al*. 2010, Baritaud *et al*. 2012, Pasupuleti et al. 2013). AIF cleavage/

nuclear translocation and γH2AX increase were not seen in PC47 cells in which VPA does not induce cell death, but the mechanism of γH2AX increase is still unclear and its interaction with tAIF remains to be documented. Consistent with the observed VPA-induced mitochondrial release of tAIF, VPA also increased the levels of Smac/DIABLO, another death associated mitochondrial protein that is released by activated calpain. This was accompanied by the inhibition of the anti-apoptotic IAP protein XIAP, an altered balance associated with necroptosis, as previously reported for Smac mimetics (McComb et al. 2012, Steinhart et al. 2013). However, additional studies are needed in order to confirm the role of the Smac/DIABLO/XIAP balance in VPA-induced cell death.

The exact role of the activated survival pathways in inhibiting VPA-induced necroptosis is still unknown, but activated ERK and Akt were previously shown to play pivotal role in VPA-mediated neuroprotection (Zhang et al. 2014). Ongoing studies are designed to better understand the mechanism of VPA-induced H2AX phosphorylation, define the mechanisms responsible for the JNK1-mediated RIP-1 expression and the role of the Smac/DIABLO/XIAP balance in VPA-induced cell death.

Additional studies are also needed in order to verify the role of these pathways in the VPA-induced death of distinct neuronal cells and different brain regions and elucidate the factors that are involved in neuroprotection in PC47 cells.

## Supplementary Material

Refer to Web version on PubMed Central for supplementary material.

## ACKNOWLEDGEMENTS

These studies were supported by grant AR053512 from the National Institute of Arthritis and Musculoskeletal and Skin Diseases.

## Abbreviations used

| | |
|---|---|
| **VPA** | valproic acid |
| **HDAC** | histone deacetylase |
| **JNK1** | c-Jun N-terminal kinase 1 |
| **RIP1** | receptor interacting protein 1 |
| **AIF** | apoptosis inducing factor |
| **IAP** | inhibitor of apoptosis |
| **XIAP** | x-linked inhibitor of apoptosis |
| **ASD** | autism spectrum disorder |
| **PCD** | programmed cell death |
| **TUNEL** | Terminal deoxynucleotidyl transferase dUTP nick end labeling |
| **FBS** | fetal bovine serum |

| | |
|---|---|
| **SDS** | sodium dodecyl sulfate |
| **PAGE** | polyacrylamide gel electrophoresis |
| **Nec-1** | necrostatin-1 |
| **NGF** | Nerve growth factor |
| **SD** | supplemental data |
| **MM** | Materials and Methods |

## REFERENCES


Arndt TL, Stodgell CJ, Rodier PM. The teratology of autism. International journal of developmental neuroscience : the official journal of the International Society for Developmental Neuroscience. 2005; 23:189–199. [PubMed: 15749245]

Artus C, Boujrad H, Bouharrour A, et al. AIF promotes chromatinolysis and caspase-independent programmed necrosis by interacting with histone H2AX. The EMBO journal. 2010; 29:1585–1599. [PubMed: 20360685]

Autheman D, Wyder M, Popoff M, D'Herde K, Christen S, Posthaus H. Clostridium perfringens beta-toxin induces necrostatin-inhibitable, calpain-dependent necrosis in primary porcine endothelial cells. PloS one. 2013; 8:e64644. [PubMed: 23734212]

Baritaud M, Boujrad H, Lorenzo HK, Krantic S, Susin SA. Histone H2AX: The missing link in AIF-mediated caspase-independent programmed necrosis. Cell cycle. 2010; 9:3166–3173. [PubMed: 20697198]

Baritaud M, Cabon L, Delavallee L, Galan-Malo P, Gilles ME, Brunelle-Navas MN, Susin SA. AIF-mediated caspase-independent necroptosis requires ATM and DNA-PK-induced histone H2AX Ser139 phosphorylation. Cell death & disease. 2012; 3:e390. [PubMed: 22972376]

Bittigau P, Sifringer M, Ikonomidou C. Antiepileptic drugs and apoptosis in the developing brain. Annals of the New York Academy of Sciences. 2003; 993:103–114. discussion 123-104. [PubMed: 12853301]

Cabon L, Galan-Malo P, Bouharrour A, Delavallee L, Brunelle-Navas MN, Lorenzo HK, Gross A, Susin SA. BID regulates AIF-mediated caspase-independent necroptosis by promoting BAX activation. Cell death and differentiation. 2012; 19:245–256. [PubMed: 21738214]

Cao G, Xing J, Xiao X, Liou AK, Gao Y, Yin XM, Clark RS, Graham SH, Chen J. Critical role of calpain I in mitochondrial release of apoptosis-inducing factor in ischemic neuronal injury. The Journal of neuroscience : the official journal of the Society for Neuroscience. 2007; 27:9278–9293. [PubMed: 17728442]

Carriere CH, Kang NH, Niles LP. Neuroprotection by valproic acid in an intrastriatal rotenone model of Parkinson's disease. Neuroscience. 2014; 267:114–121. [PubMed: 24613722]

Chateauvieux S, Morceau F, Dicato M, Diederich M. Molecular and therapeutic potential and toxicity of valproic acid. Journal of biomedicine & biotechnology. 2010; 2010

Chaudhary S, Parvez S. An in vitro approach to assess the neurotoxicity of valproic acid-induced oxidative stress in cerebellum and cerebral cortex of young rats. Neuroscience. 2012; 225:258–268. [PubMed: 22960313]

Chen S, Wu H, Klebe D, Hong Y, Zhang J. Valproic Acid: A New Candidate of Therapeutic Application for the Acute Central Nervous System Injuries. Neurochemical research. 2014

Chiu CT, Wang Z, Hunsberger JG, Chuang DM. Therapeutic potential of mood stabilizers lithium and valproic acid: beyond bipolar disorder. Pharmacological reviews. 2013; 65:105–142. [PubMed: 23300133]

Cho YS, Challa S, Moquin D, Genga R, Ray TD, Guildford M, Chan FK. Phosphorylation-driven assembly of the RIP1-RIP3 complex regulates programmed necrosis and virus-induced inflammation. Cell. 2009; 137:1112–1123. [PubMed: 19524513]

Christensen J, Gronborg TK, Sorensen MJ, Schendel D, Parner ET, Pedersen LH, Vestergaard M. Prenatal valproate exposure and risk of autism spectrum disorders and childhood autism. JAMA : the journal of the American Medical Association. 2013; 309:1696–1703.

Christofferson DE, Li Y, Hitomi J, Zhou W, Upperman C, Zhu H, Gerber SA, Gygi S, Yuan J. A novel role for RIP1 kinase in mediating TNFalpha production. Cell death & disease. 2012; 3:e320. [PubMed: 22695613]

Coffey ET. Nuclear and cytosolic JNK signalling in neurons. Nature reviews. Neuroscience. 2014; 15:285–299.

Danial NN, Korsmeyer SJ. Cell death: critical control points. Cell. 2004; 116:205–219. [PubMed: 14744432]

Degterev A, Hitomi J, Germscheid M, et al. Identification of RIP1 kinase as a specific cellular target of necrostatins. Nature chemical biology. 2008; 4:313–321.

Delavallee L, Cabon L, Galan-Malo P, Lorenzo HK, Susin SA. AIF-mediated caspase-independent necroptosis: a new chance for targeted therapeutics. IUBMB life. 2011; 63:221–232. [PubMed: 21438113]

Douglas DL, Baines CP. PARP1-mediated necrosis is dependent on parallel JNK and Ca(2)(+)/calpain pathways. Journal of cell science. 2014; 127:4134–4145. [PubMed: 25052090]

Dragunow M, Greenwood JM, Cameron RE, Narayan PJ, O'Carroll SJ, Pearson AG, Gibbons HM. Valproic acid induces caspase 3-mediated apoptosis in microglial cells. Neuroscience. 2006; 140:1149–1156. [PubMed: 16600518]

Festjens N, Vanden Berghe T, Cornelis S, Vandenabeele P. RIP1, a kinase on the crossroads of a cell's decision to live or die. Cell death and differentiation. 2007; 14:400–410. [PubMed: 17301840]

Forgione N, Tropepe V. Histone deacetylase inhibition promotes Caspase-independent cell death of ventral midbrain neurons. Molecular and cellular neurosciences. 2011; 48:117–128. [PubMed: 21763771]

Francois F, Godinho MJ, Dragunow M, Grimes ML. A population of PC12 cells that is initiating apoptosis can be rescued by nerve growth factor. Molecular and cellular neurosciences. 2001; 18:347–362. [PubMed: 11640893]

Fujiki R, Sato A, Fujitani M, Yamashita T. A proapoptotic effect of valproic acid on progenitors of embryonic stem cell-derived glutamatergic neurons. Cell death & disease. 2013; 4:e677. [PubMed: 23788034]

Gober MD, Laing JM, Thompson SM, Aurelian L. The growth compromised HSV-2 mutant DeltaRR prevents kainic acid-induced apoptosis and loss of function in organotypic hippocampal cultures. Brain research. 2006; 1119:26–39. [PubMed: 17020750]

Golembewski EK, Wales SQ, Aurelian L, Yarowsky PJ. The HSV-2 protein ICP10PK prevents neuronal apoptosis and loss of function in an in vivo model of neurodegeneration associated with glutamate excitotoxicity. Experimental neurology. 2007; 203:381–393. [PubMed: 17046754]

Goll DE, Thompson VF, Li H, Wei W, Cong J. The calpain system. Physiological reviews. 2003; 83:731–801. [PubMed: 12843408]

Green DR. Apoptotic pathways: paper wraps stone blunts scissors. Cell. 2000; 102:1–4. [PubMed: 10929706]

Haeusgen W, Boehm R, Zhao Y, Herdegen T, Waetzig V. Specific activities of individual c-Jun N-terminal kinases in the brain. Neuroscience. 2009; 161:951–959. [PubMed: 19364525]

Han BR, You BR, Park WH. Valproic acid inhibits the growth of HeLa cervical cancer cells via caspase-dependent apoptosis. Oncology reports. 2013; 30:2999–3005. [PubMed: 24064712]

Han W, Xie J, Fang Y, Wang Z, Pan H. Nec-1 Enhances Shikonin-Induced Apoptosis in Leukemia Cells by Inhibition of RIP-1 and ERK1/2. International journal of molecular sciences. 2012; 13:7212–7225. [PubMed: 22837689]

Hirsch B, von der Wall E, Hummel M, Durkop H. RIP1 expression is necessary for CD30-mediated cell death induction in anaplastic large-cell lymphoma cells. Laboratory investigation; a journal of technical methods and pathology. 2013; 93:677–689.

Huang Y, Li X, Wang Y, Wang H, Huang C, Li J. Endoplasmic reticulum stress-induced hepatic stellate cell apoptosis through calcium-mediated JNK/P38 MAPK and Calpain/Caspase-12 pathways. Molecular and cellular biochemistry. 2014; 394:1–12. [PubMed: 24961950]

Ingram JL, Peckham SM, Tisdale B, Rodier PM. Prenatal exposure of rats to valproic acid reproduces the cerebellar anomalies associated with autism. Neurotoxicology and teratology. 2000; 22:319–324. [PubMed: 10840175]

Jin N, Kovacs AD, Sui Z, Dewhurst S, Maggirwar SB. Opposite effects of lithium and valproic acid on trophic factor deprivation-induced glycogen synthase kinase-3 activation, c-Jun expression and neuronal cell death. Neuropharmacology. 2005; 48:576–583. [PubMed: 15755485]

Johannessen CU. Mechanisms of action of valproate: a commentatory. Neurochemistry international. 2000; 37:103–110. [PubMed: 10812195]

Kanai H, Sawa A, Chen RW, Leeds P, Chuang DM. Valproic acid inhibits histone deacetylase activity and suppresses excitotoxicity-induced GAPDH nuclear accumulation and apoptotic death in neurons. The pharmacogenomics journal. 2004; 4:336–344. [PubMed: 15289798]

Lai TW, Zhang S, Wang YT. Excitotoxicity and stroke: identifying novel targets for neuroprotection. Progress in neurobiology. 2014; 115:157–188. [PubMed: 24361499]

Laing JM, Gober MD, Golembewski EK, Thompson SM, Gyure KA, Yarowsky PJ, Aurelian L. Intranasal administration of the growth-compromised HSV-2 vector DeltaRR prevents kainate-induced seizures and neuronal loss in rats and mice. Molecular therapy : the journal of the American Society of Gene Therapy. 2006; 13:870–881. [PubMed: 16500153]

Leng Y, Liang MH, Ren M, Marinova Z, Leeds P, Chuang DM. Synergistic neuroprotective effects of lithium and valproic acid or other histone deacetylase inhibitors in neurons: roles of glycogen synthase kinase-3 inhibition. The Journal of neuroscience : the official journal of the Society for Neuroscience. 2008; 28:2576–2588. [PubMed: 18322101]

Lin Y, Devin A, Rodriguez Y, Liu ZG. Cleavage of the death domain kinase RIP by caspase-8 prompts TNF-induced apoptosis. Genes & development. 1999; 13:2514–2526. [PubMed: 10521396]

Loscher W. Basic pharmacology of valproate: a review after 35 years of clinical use for the treatment of epilepsy. CNS drugs. 2002; 16:669–694. [PubMed: 12269861]

Mahadeo D, Kaplan L, Chao MV, Hempstead BL. High affinity nerve growth factor binding displays a faster rate of association than p140trk binding. Implications for multi-subunit polypeptide receptors. The Journal of biological chemistry. 1994; 269:6884–6891. [PubMed: 8120051]

McComb S, Cheung HH, Korneluk RG, Wang S, Krishnan L, Sad S. cIAP1 and cIAP2 limit macrophage necroptosis by inhibiting Rip1 and Rip3 activation. Cell death and differentiation. 2012; 19:1791–1801. [PubMed: 22576661]

Mielke K, Damm A, Yang DD, Herdegen T. Selective expression of JNK isoforms and stress-specific JNK activity in different neural cell lines. Brain research. Molecular brain research. 2000; 75:128–137. [PubMed: 10648896]

Morizane Y, Honda R, Fukami K, Yasuda H. X-linked inhibitor of apoptosis functions as ubiquitin ligase toward mature caspase-9 and cytosolic Smac/DIABLO. Journal of biochemistry. 2005; 137:125–132. [PubMed: 15749826]

Ornoy A. Valproic acid in pregnancy: how much are we endangering the embryo and fetus? Reproductive toxicology. 2009; 28:1–10. [PubMed: 19490988]

Pasupuleti N, Leon L, Carraway KL 3rd, Gorin F. 5-Benzylglycinyl-amiloride kills proliferating and nonproliferating malignant glioma cells through caspase-independent necroptosis mediated by apoptosis-inducing factor. The Journal of pharmacology and experimental therapeutics. 2013; 344:600–615. [PubMed: 23241369]

Perkins D, Pereira EF, Aurelian L. The herpes simplex virus type 2 R1 protein kinase (ICP10 PK) functions as a dominant regulator of apoptosis in hippocampal neurons involving activation of the ERK survival pathway and upregulation of the antiapoptotic protein Bag-1. Journal of virology. 2003; 77:1292–1305. [PubMed: 12502846]

Reinecke K, Herdegen T, Eminel S, Aldenhoff JB, Schiffelholz T. Knockout of c-Jun N-terminal kinases 1, 2 or 3 isoforms induces behavioural changes. Behavioural brain research. 2013; 245:88–95. [PubMed: 23428746]

Sano M, Nishiyama K, Kitajima S. A nerve growth factor-dependent protein kinase that phosphorylates microtubule-associated proteins in vitro: possible involvement of its activity in the

outgrowth of neurites from PC12 cells. Journal of neurochemistry. 1990; 55:427–435. [PubMed: 2164566]

Sevrioukova IF. Apoptosis-inducing factor: structure, function, and redox regulation. Antioxidants & redox signaling. 2011; 14:2545–2579. [PubMed: 20868295]

Shah RD, Jagtap JC, Mruthyunjaya S, Shelke GV, Pujari R, Das G, Shastry P. Sodium valproate potentiates staurosporine-induced apoptosis in neuroblastoma cells via Akt/survivin independently of HDAC inhibition. Journal of cellular biochemistry. 2013; 114:854–863. [PubMed: 23097134]

Sheikh AM, Li X, Wen G, Tauqeer Z, Brown WT, Malik M. Cathepsin D and apoptosis related proteins are elevated in the brain of autistic subjects. Neuroscience. 2010a; 165:363–370. [PubMed: 19854241]

Sheikh AM, Malik M, Wen G, Chauhan A, Chauhan V, Gong CX, Liu F, Brown WT, Li X. BDNF-Akt-Bcl2 antiapoptotic signaling pathway is compromised in the brain of autistic subjects. Journal of neuroscience research. 2010b; 88:2641–2647. [PubMed: 20648653]

Steinhart L, Belz K, Fulda S. Smac mimetic and demethylating agents synergistically trigger cell death in acute myeloid leukemia cells and overcome apoptosis resistance by inducing necroptosis. Cell death & disease. 2013; 4:e802. [PubMed: 24030154]

Stockhausen MT, Sjolund J, Manetopoulos C, Axelson H. Effects of the histone deacetylase inhibitor valproic acid on Notch signalling in human neuroblastoma cells. British journal of cancer. 2005; 92:751–759. [PubMed: 15685243]

Storr SJ, Carragher NO, Frame MC, Parr T, Martin SG. The calpain system and cancer. Nature reviews. Cancer. 2011; 11:364–374.

Tan Y, Dourdin N, Wu C, De Veyra T, Elce JS, Greer PA. Ubiquitous calpains promote caspase-12 and JNK activation during endoplasmic reticulum stress-induced apoptosis. The Journal of biological chemistry. 2006; 281:16016–16024. [PubMed: 16597616]

Tung EW, Winn LM. Valproic acid increases formation of reactive oxygen species and induces apoptosis in postimplantation embryos: a role for oxidative stress in valproic acid-induced neural tube defects. Molecular pharmacology. 2011; 80:979–987. [PubMed: 21868484]

Umka J, Mustafa S, ElBeltagy M, Thorpe A, Latif L, Bennett G, Wigmore PM. Valproic acid reduces spatial working memory and cell proliferation in the hippocampus. Neuroscience. 2010; 166:15–22. [PubMed: 20006675]

Valavanis C, Hu Y, Yang Y, Osborne BA, Chouaib S, Greene L, Ashwell JD, Schwartz LM. Model cell lines for the study of apoptosis in vitro. Methods in cell biology. 2001; 66:417–436. [PubMed: 11396014]

Vandenabeele P, Declercq W, Van Herreweghe F, Vanden Berghe T. The role of the kinases RIP1 and RIP3 in TNF-induced necrosis. Science signaling. 2010; 3:re4. [PubMed: 20354226]

Waetzig V, Herdegen T. A single c-Jun N-terminal kinase isoform (JNK3-p54) is an effector in both neuronal differentiation and cell death. The Journal of biological chemistry. 2003; 278:567–572. [PubMed: 12401814]

Wales SQ, Laing JM, Chen L, Aurelian L. ICP10PK inhibits calpain-dependent release of apoptosis-inducing factor and programmed cell death in response to the toxin MPP+ Gene therapy. 2008; 15:1397–1409. [PubMed: 18496573]

Wang C, Luan Z, Yang Y, Wang Z, Cui Y, Gu G. Valproic acid induces apoptosis in differentiating hippocampal neurons by the release of tumor necrosis factor-alpha from activated astrocytes. Neuroscience letters. 2011; 497:122–127. [PubMed: 21543053]

Xiong S, Mu T, Wang G, Jiang X. Mitochondria-mediated apoptosis in mammals. Protein & cell. 2014; 5:737–749. [PubMed: 25073422]

Yochum CL, Dowling P, Reuhl KR, Wagner GC, Ming X. VPA-induced apoptosis and behavioral deficits in neonatal mice. Brain research. 2008; 1203:126–132. [PubMed: 18316065]

Zhang C, Zhu J, Zhang J, et al. Neuroprotective and anti-apoptotic effects of valproic acid on adult rat cerebral cortex through ERK and Akt signaling pathway at acute phase of traumatic brain injury. Brain research. 2014

Zhao Y, Spigolon G, Bonny C, Culman J, Vercelli A, Herdegen T. The JNK inhibitor D-JNKI-1 blocks apoptotic JNK signaling in brain mitochondria. Molecular and cellular neurosciences. 2012; 49:300–310. [PubMed: 22206897]

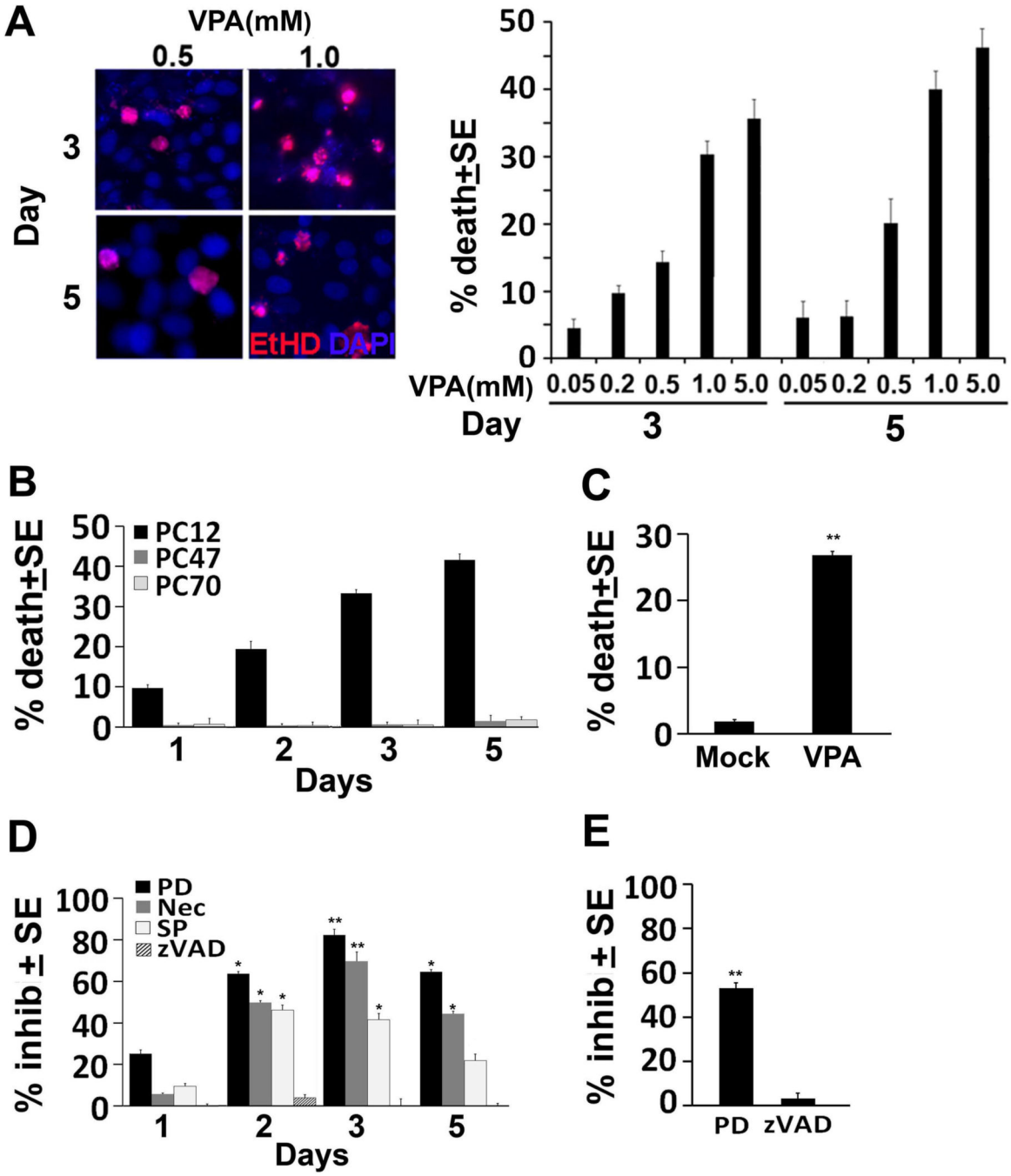


**Figure 1. VPA induces neuronal cell death; inhibited by calpain, JNK and necroptosis inhibitors**

**(A)** PC12 cells neuronally differentiated as described in MM were treated with VPA (0.05, 0.2, 0.5, 1, 5mM), and assayed for cell death by ethidium homodimer staining 3 and 5 days later. Dead cells (red staining) were counted in 4 quadrants and the % dead cells was calculated and normalized to untreated cells. The results are expressed as % death cells ± SE. **(B)** PC12, PC70, and PC47 cells were differentiated as in **(A)**. They were treated with VPA (1mM) and assayed for cell death by trypan blue exclusion 1, 2, 3, and 5 days later. Dead cells (blue staining) were counted in 4 quadrants and the % dead cells was calculated

and normalized to untreated cells. The results are expressed as % trypan blue+ cells ± SE. **(C)** Primary rat cortex neurons were mock or VPA (1mM)-treated and assayed for cell death by trypan blue staining 3 days post-treatment. Dead and live cells were counted as in **(B)** and the % dead cells was calculated and normalized to untreated cells. **(D)** PC12 cells cultured and differentiated as in **(A)** were treated with VPA (1mM) alone or with z-VAD-fmk (50 μM), PD150606 (PD, 100 μM), SP600125 (SP, 100 μM) or Nec-1 (Nec, 50 μM) and assayed for cell death by trypan blue exclusion at 1,2,3,and 5 days post-treatment. Dead and live cells were counted as in **(B)** and the % dead cells was calculated and normalized to untreated cells. The results are expressed as % inhibition ± SE calculated from the formula: 100-((% death with inhibitors/% death without inhibitors) ×100). Maximal inhibitory levels were reached on day 3 post-treatment as determined by one-way ANOVA. **(E)** Primary rat cortex neuronal cells were treated with VPA (1mM) alone or in the presence of z-VAD-fmk (50 μM) or PD150606 (PD, 100 μM) and assayed for cell death by trypan blue 3 days post-treatment. Dead and live cells were counted as in **(B)** and the % dead cells was calculated and normalized to untreated cells. The results are expressed as % inhibition ± SE, calculated as in **(D)**. (*P<0.01; **P<0.001)

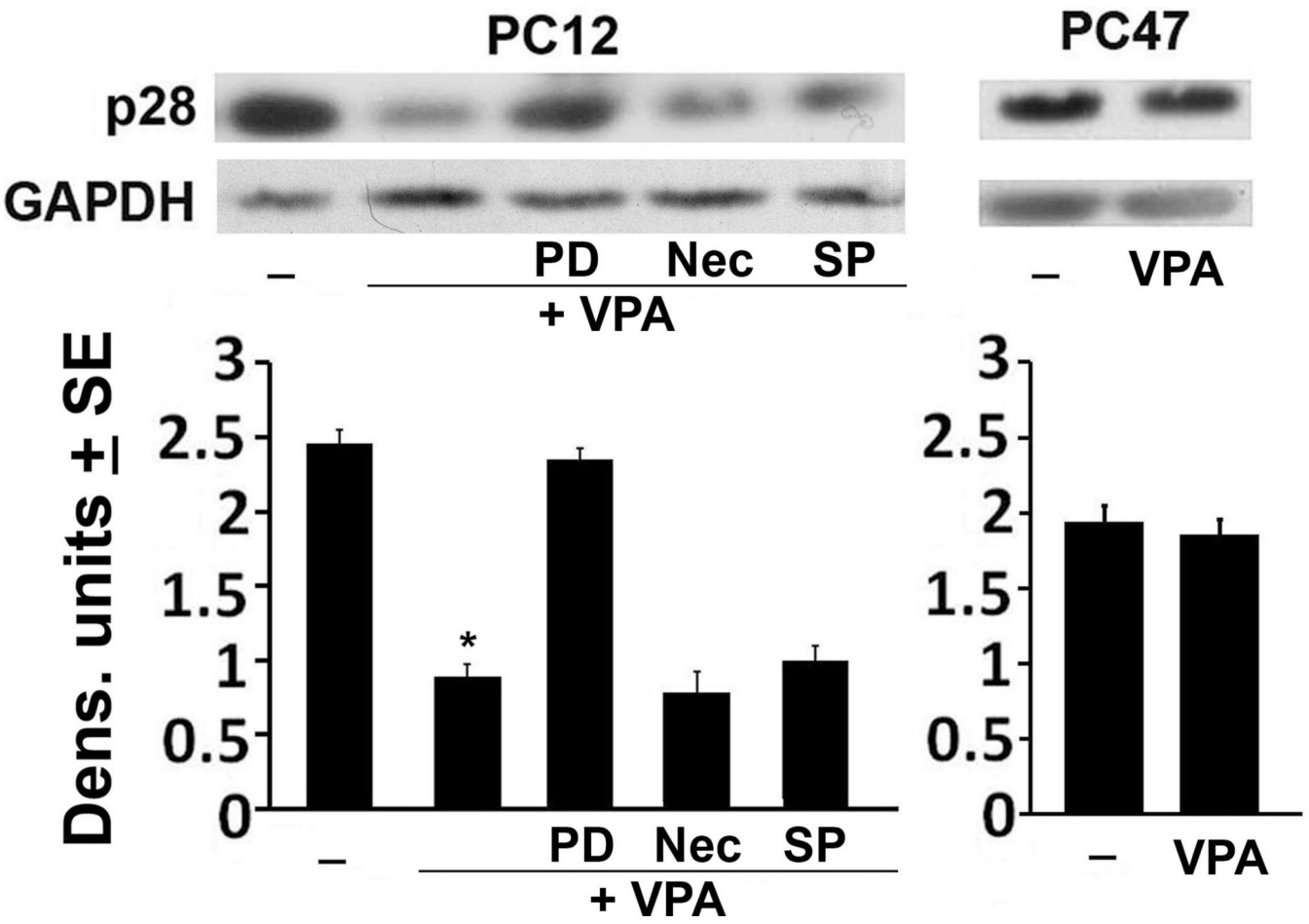


**Figure 2. Calpain is activated in VPA-treated PC12, but not PC47 cells**

Neuronally differentiated PC12 and PC47 cells were mock- or VPA (1mM)-treated alone or in combination with PD, SP or Nec as Fig. 1B. Cell extracts obtained 48hrs post treatment were immunoblotted with antibody to the calpain p28 regulatory subunit. The blots were stripped and re-probed with antibody to GAPDH. Data were quantified by densitometric scanning and are expressed as densitometric units ± SE. (*P<0.001, by one-way ANOVA).

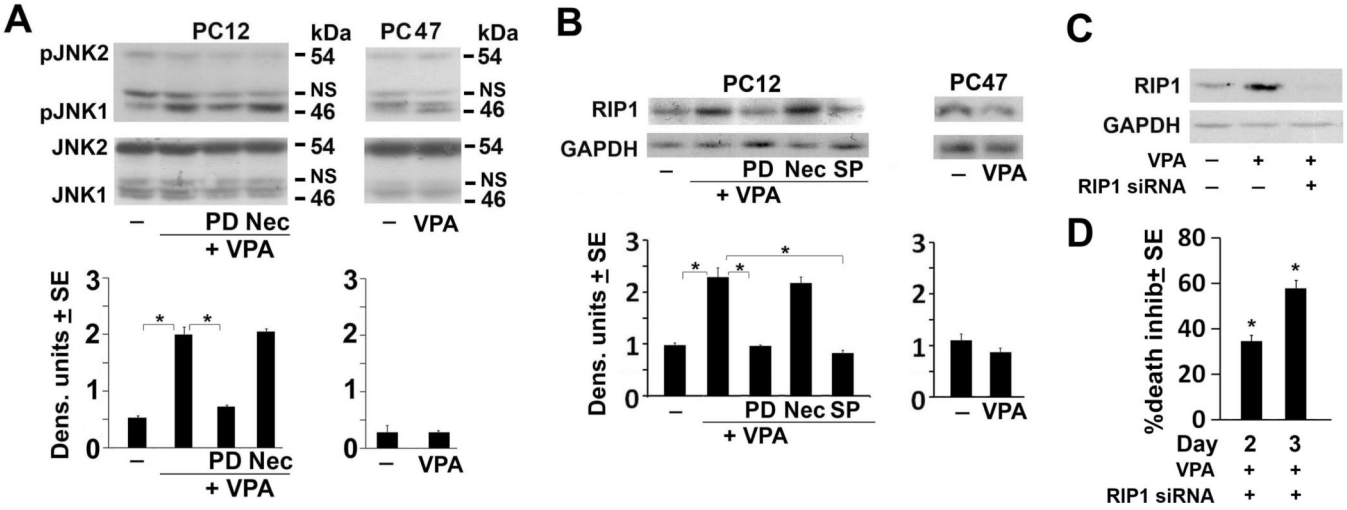


**Figure 3. VPA activates JNK1, leading to increased RIP-1 expression**

**(A)** Neuronally differentiated PC12 and PC47 cells were mock- or VPA (1mM)-treated alone or in combination with PD or Nec as in Fig. 1B. Cell extracts obtained at 48hrs post treatment were immunoblotted with antibody to phosphorylated JNK1 (pJNK1, p46) and JNK2 (pJNK2, p54) and the blots were stripped and re-probed with antibody to total JNK1/2 or GAPDH. Data were quantified by densitometric scanning and the results are expressed as densitometric units ± SE. NS = non-specific. **(B)** Duplicates of the PC12 and PC47 cultures were mock or VPA-treated alone or together with PD, SP or Nec as in Fig. 1B, and cell extracts collected at 48hrs post-treatment were immunoblotted with RIP-1 antibody. Blots were stripped and re-probed with antibody to GAPDH. **(C)** PC12 cells were differentiated and transfected with vehicle or RIP-1 siRNA as described in MM. Two days later, the cells were mock or VPA treated and cell extracts collected 2 days later were immunoblotted with RIP-1 antibody. The blots were stripped and re-probed with antibody to GAPDH. **(D)** Duplicates of similarly treated PC12 cultures were assayed for cell death using trypan blue staining at 2 and 3 days post VPA treatment. Dead cells (blue staining) were counted in 4 quadrants and the % was calculated and normalized to untreated cells. The results are expressed as % inhibition SE calculated as in Fig 1D. (*P< 0.001 by one-way ANOVA).

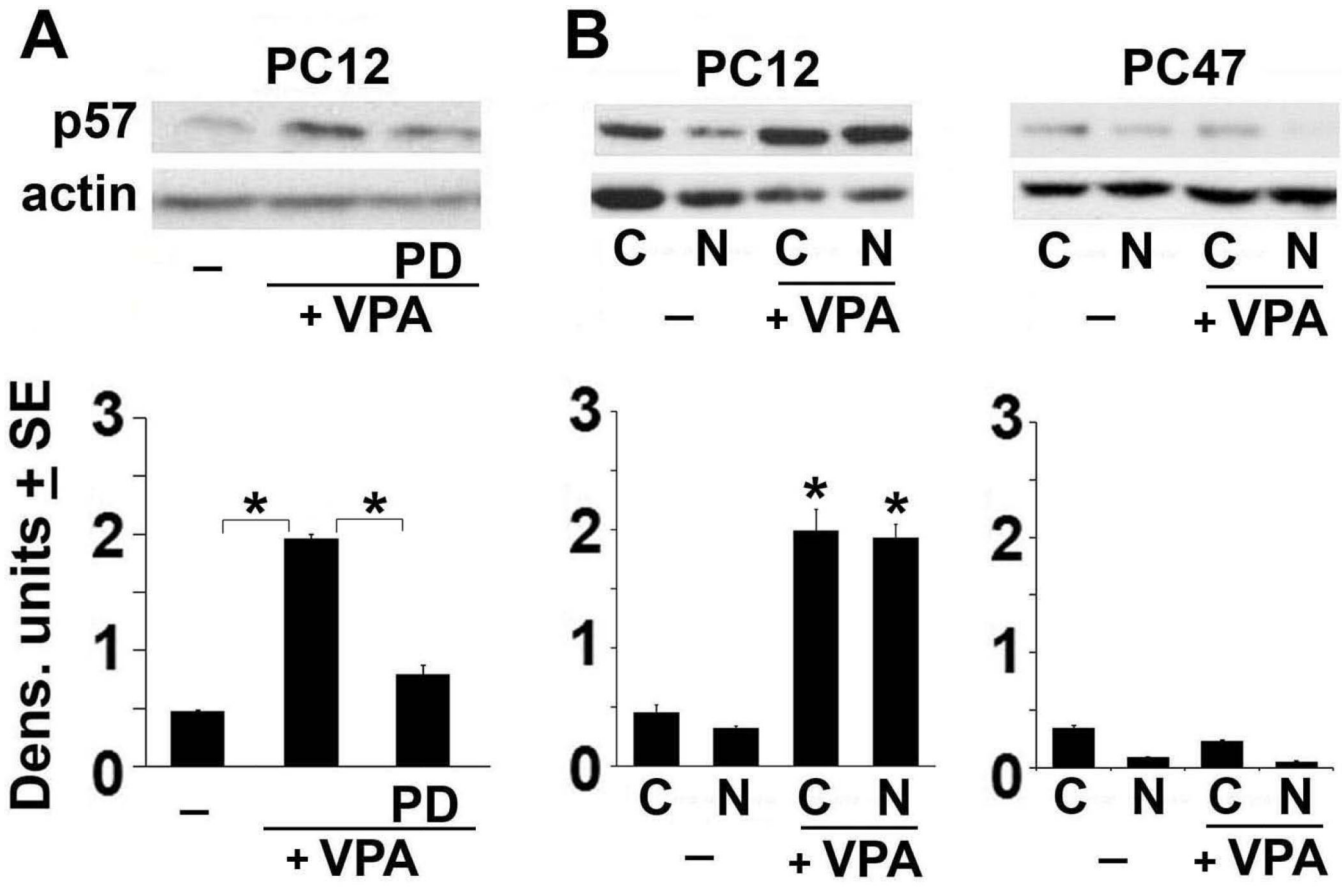


**Figure 4. VPA induces AIF cleavage to a 57 kDa (tAIF) band and promotes its nuclear translocation**

**(A)** Neuronally differentiated PC12 cells were differentiated and mock- or VPA (1mM)-treated alone or in combination with PD as in Fig. 1B and whole cell extracts collected 72 hrs post-treatment were immunoblotted with AIF antibody. Data were quantified using densitometric scanning and are expressed as densitometric units ± SE. The levels of the 57kDa (tAIF) band were increased by VPA treatment and restored to those in mock-treated cells by PD treatment. **(B)** Neuronally differentiated PC12 and PC47 cells were mock- or VPA-treated as in Fig. 1 and cell extracts obtained 72 hrs post treatment were fractionated into nuclear (N) and cytoplasmic (C) fractions as described in MM. The fractions were immunoblotted with AIF antibody and the blots were stripped and re-probed with antibody to β-actin. Data were quantified by densitometric scanning and the results are expressed as densitometric units ± SE. The levels of the 57kDa tAIF band were significantly increased in both the cytoplasmic and nuclear fractions from the VPA-treated PC12, but not PC47 cells. (*P<0.001 by one-way ANOVA).

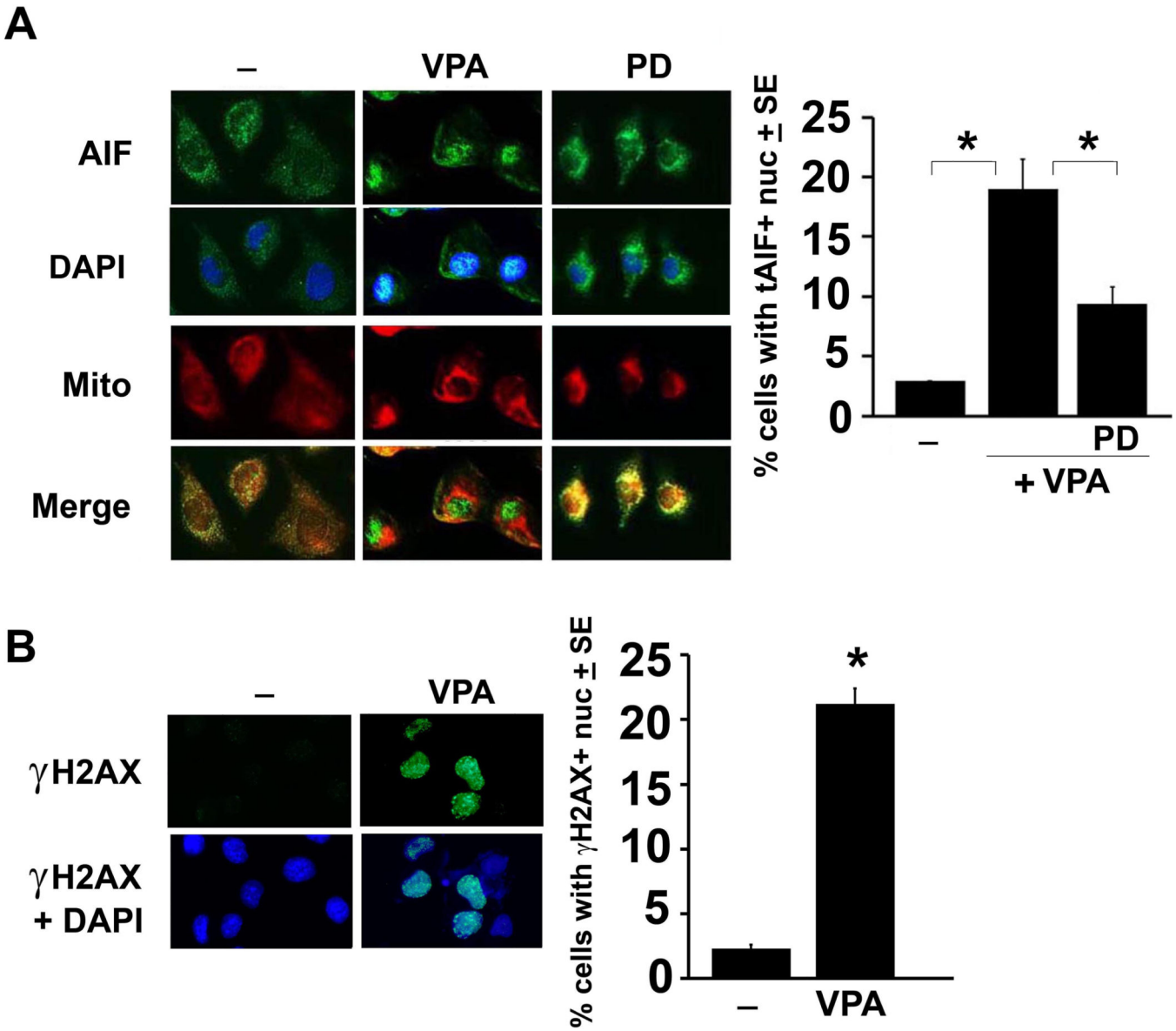


**Figure 5. VPA induces tAIF mitochondrial release and increases levels of γH2AX**

**(A)** Neuronally differentiated PC12 cells were mock- or VPA-treated alone or with PD as described in Fig. 1B. Coverslips obtained at 72hrs post-treatment were incubated with MitoTracker Red 580 and stained with AIF antibody (green), as described in MM. Cells with AIF nuclear staining were counted in 4 randomly chosen fields and the % staining cells was calculated relative to total cell numbers, identified by DAPI staining. Results are expressed as % cells with tAIF+ nuclear staining ± SE. VPA caused a significant increase in the number of cells with AIF nuclear localization, inhibited by PD (*P≤ 0.01 by one-way ANOVA). **(B)** Duplicates of the mock- and VPA-treated PC12 cultures were stained with antibody to H2AX (green) and DAPI (blue) used to visualize the nuclei. Cells with H2AX nuclear staining were counted and the % calculated relative to total cell numbers as in **(A)**. The results are expressed as % cells with H2AX + nuclear staining ± SE. (*P<0.01 by one-way ANOVA).

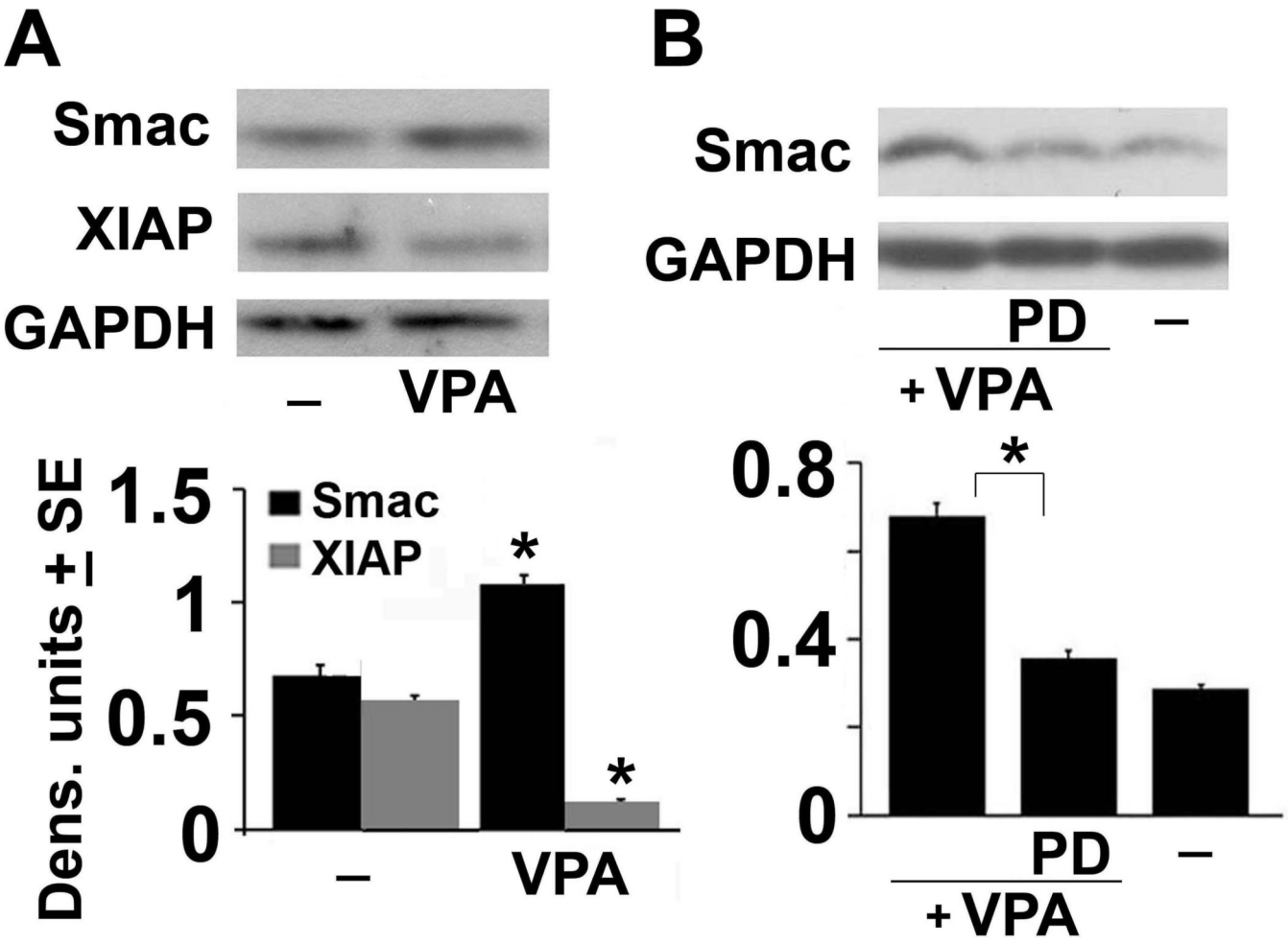


**Figure 6. VPA increases Smac/DIABLO and decreases XIAP**

**(A)** Neuronally differentiated PC12 cells were mock- or VPA-treated as in Fig. 1 and cell extracts obtained 72 hrs post-treatment were immunoblotted with antibody to Smac/DIABLO. The blots were stripped and re-probed with antibody to XIAP followed by GAPDH. Data were quantified using densitometric scanning and are expressed as densitometric units ± SE. **(B)** Duplicate cultures of PC12 cells were mock or VPA-treated alone or together with PD as in Fig. 1B and cells extracts were immunoblotted with Smac/DIABLO antibody. The blot was stripped and re-probed with antibody to GAPDH and the data were quantified by densitometric scanning. Results are expressed as densitometric units ± SE. (*P< 0.001 by one-way ANOVA).

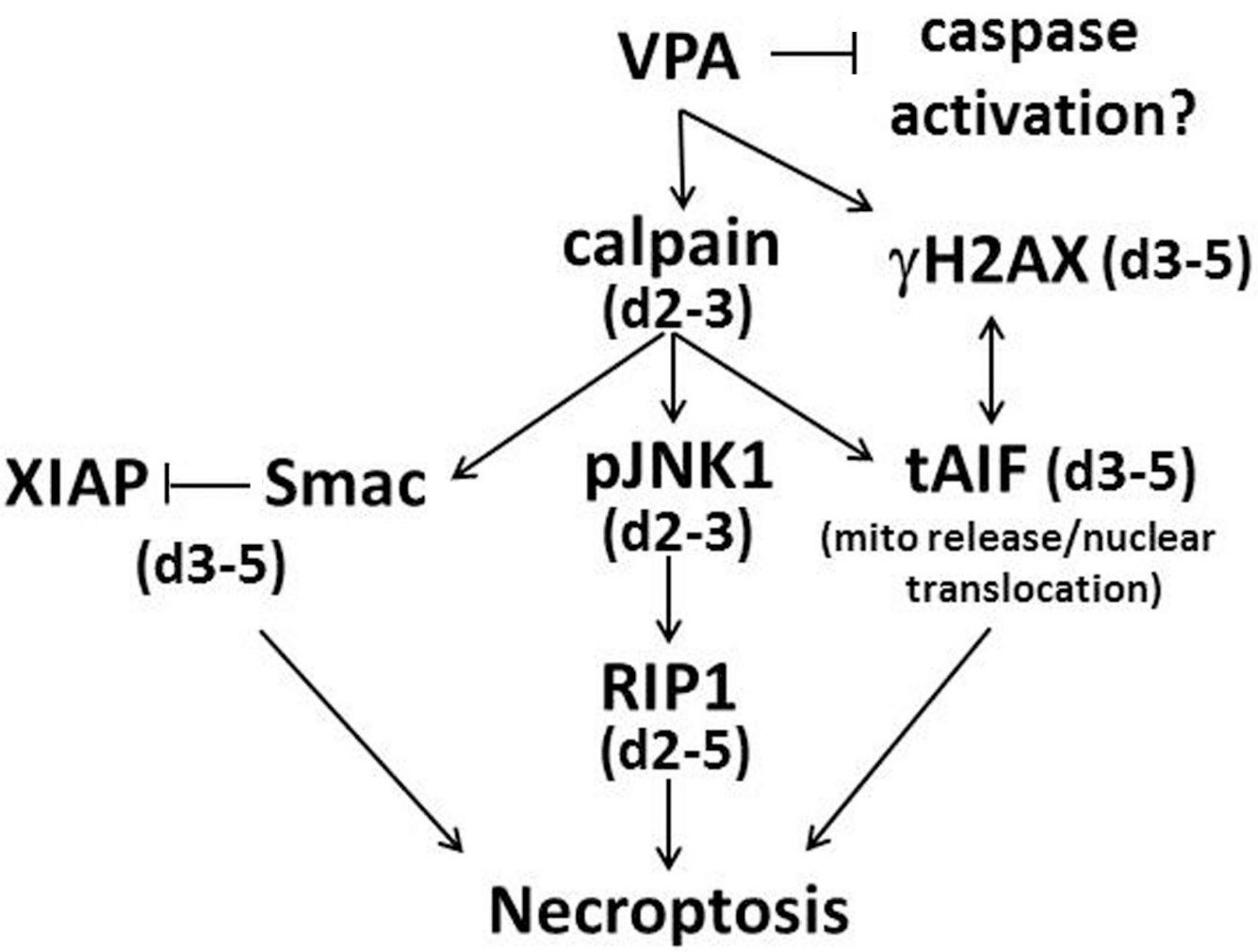


**Figure 7. Schematic representation of VPA-induced neuronal cell death**

Our data confirm a VPA-induced necroptotic pathway that initiates with calpain activation and is accompanied by calpain-dependent activation of JNK1, which is responsible for increased RIP-1 expression. Calpain induces Smac/DIABLO expression as well as cleavage and nuclear translocation of AIF. VPA increases nuclear H2AX, which can complex with tAIF to promote chromatinolysis and necroptotic cell death. Smac/DIABLO increase is accompanied by reduced expression of XIAP, further contributing to necroptosis. These pathways are not activated in PC47 cells that have constitutively activated survival pathways. D= days post-VPA-treatment.